Reaction Kinetics, Mechanisms and Catalysis (2024) 137:2431–2449
https://doi.org/10.1007/s11144-024-02648-4

Development of a new magnetic mesoporous activated carbon for the photocatalytic degradation of basic red 18 and reactive red 180 dyes under UVA radiation

Badis Bouider[1] · Kamel Rida[1] · Aya Alterkaoui[2] · Zelal Isik[2] · Nadir Dizge[2]

Received: 25 March 2024 / Accepted: 10 May 2024 / Published online: 1 June 2024

Abstract
In this study, the UVA-induced degradation of Basic Red 18 and Reactive Red 180 was examined using a photocatalytic treatment system using magnetic activated carbon derived from the fruit rind of *Brachychiton populneus*. Numerous factors, including the pH of the solution, the dose of photocatalyst, and the initial concentration of the dye, have been optimized because they affect the photocatalytic activity of magnetic activated carbon.The pH of the solution (6 for basic Red 18 and reactive red 180) and 0.75 g L^{-1} of magnetic activated carbon with a degradation rate of 100% and 82% for Basic Red 18 and Reactive Red 180, respectively, are the parameters that should be set at their optimal values for an initial dye concentration of 50 mg L^{-1}. Superoxide and electrons are the main active species and play a major role in the photocatalytic degradation of dyes by magnetic activated carbon under UVA light irradiation. The two dyes had five cycles of reuse, according to a study on magnetic activated carbon that was completed under optimal conditions.

Keywords Magnetic activated carbon · *Brachychiton populneus* · Photocatalysis · Basic Red 18 · Reactive Red 180 · Reuse

Introduction

Massive issues with the environment and human health have been brought on by modern industrialization and technological advancement. Water contamination has been among the effects of these issues, harming the ecosystem and

✉ Kamel Rida
rida_kamel2001@yahoo.fr

[1] Laboratoire d'interaction Matériaux et Environnement (LIME), Faculté des Sciences et de la Technologie, Université de Jijel, 18000 Jijel, Algeria

[2] Department of Environmental Engineering, Mersin University, 33343 Mersin, Turkey

endangering the human population [1]. These contaminants are plentiful in the environment, non-biodegradable, poisonous, persistent, and carcinogenic [2].

Polluted wastewater, especially from textiles [3], is typically treated using physical or chemical methods, such as photocatalysis [4], ozonation [5], and adsorption [6]. Among the most crucial chemical approaches for wastewater treatment, photocatalysis is one of the most important processes. Recent years have seen a great interest in photocatalytic reactions as efficient approaches to treating wastewater from many industries [7, 8]. In comparison to other wastewater treatment technologies like adsorption, these methods are more efficient, environmentally benign, and achieve high quality water by limiting wastewater concentration without producing photocatalytic degradation or secondary pollutants [4]. The ability of oxygen species in air and water molecules to mineralize organic contaminants allows them to be used as chemical compounds in the photocatalytic process, which produces entirely nontoxic molecules [9]. In recent years, photocatalytic reactions have used a lot of semiconductor materials as catalysts, such as ZnO, TiO_2, CdS, and Fe_3O_4 [10–14]. On the other hand, reactions involving the different semiconductor materials might also cause issues. In this regard, using conventional semiconductor materials has serious limitations including challenging photocatalyst final separation [15, 16]. To address these issuesand inconveniences, scientists therefore set out to identify an appropriate replacement for semiconductor materials [17]. For photocatalytic operations, it is crucial to employ economical photocatalysts. It is also advantageous to use photocatalysts made from organic and inorganic waste. Magnetic activated carbon nanoparticles are being investigated as the new generation of photocatalyst for water treatment due to the degradation of water quality [18]. Due to its excellent magnetic properties, high biocompatibility, easy separation using an external magnetic field, reuse, and relatively low cost, magnetic activated carbon makes an excellent photocatalyst [19, 20].

With the recovery of various wastes and biomass, such as coconut shell [21] and peanut shell [22], which were generated by impregnating them with varying ratios of ferric chloride ($FeCl_3{\cdot}6H_2O$). Magnetic activated carbon can be made from a variety of high carbon precursors. Due to its low cost, high carbon content, and accessibility, this study exploited the shell of the Mediterranean species Brachychiton populneus as the new precursor for the production of magnetic activated carbon. To our knowledge, there hasn't been any research on using these nuclei as the source of activated carbon and using it to degrade colors in the aqueous phase by photocatalysis.

This study aims to use magnetic activated carbon obtained by impregnation of the fruit's shell of the Brachychiton Populneus plant in the $FeCl_3{\cdot}6H_2O$ solution as a photocatalyst. Under a UVA light source, the photocatalytic degradation of two distinct dyes, the anionic Reactive Red 180 and the cationic Basic Red 18, was observed. The investigation examined the optimisation of he experimental conditions for the photocatalytic processus such as catalyst concentration, initial dye concentration, and pH. Carry out a study to identify the reactive species responsible in the mechanism of photocatalytic degradation of dyes under UVA light irradiation. Furthermore investigated was the reuse of magnetic activated carbon under the optimal conditions established for the two types of dyes.

Materials and methods

Materials

The fruit rind of Brachychiton populneus is collected in the region of Jijel (Eastern Algeria). Analytical-grade chemicals and reagents were all provided by Sigma–Aldrich (Germany) for the investigation. Iron chloride ($FeCl_3 \cdot 6H_2O$, 96%), hydrochloric acid (HCl, 37%), sodium hydroxide (NaOH, 98%), silver nitrate ($AgNO_3$, 98%), ethylene diamine tetraacetate (EDTA, 99%), isopropanol (IPA, 99%), ascorbic acid (ASC, 99%). A cationic dye basic red 18 (BR18) and an anionic dye reactive red 180 (RR180), their characteristics and chemical formula are listed in Table 1.

Preparation of magnetic activated carbon (MAC)

Activated carbon is prepared from a biomass that is collected in the region of Jijel (Eastern Algeria), it is the crust of the fruit of a tree called *Brachychiton populneus*, it is a solid colored biomass dark brown and oval in shape as shown in Fig. S1. The magnetic activated carbon preparation protocol has been described in detail in recently published article [6], after being cleaned, the biomass is chopped into pieces and air dried. After being carbonized for 2 h at a temperature of 300 °C in a muffle furnace, the biomass was extensively ground in an agate mortar. Chemical activation is carried out by iron chlorides ($FeCl_3 \cdot 6H_2O$) at a temperature between 60 and 80 °C for 4 h in reflus. The resulting carbon is then repeatedly rinsed with distilled water until rinse water with a pH of between 6 and 7 is achieved, and dried in an oven at 105 °C for 24 h. The activated carbon undergoes pyrolysis in a tubular oven under steam at 800 °C for 90 min in order to develop the physical and chemical properties (Fig. S2).

Characterization methods

Analysis of X-ray diffraction (XRD; Bruker, D8 Venture) was utilized to investigate the crystal structure and crystallographic properties of MAC. With the use of an EDX study, the surface morphology of the MAC was determined and investigated with a scanning electron microscope (SEM; Zeiss Supra 55/Germany). The specific surface, the volume of the pores and the average diameter of the pores were determined using

Table 1 Physico–chemical characteristics of the dyes studied

Chemical name	Basic Red 18 (BR18)	Reactive Red 180 (RR180)
Chemical formula	$C_{19}H_{25}ClN_5O_2$	$C_{29}H_{19}N_3Na_4O_{17}S_5$
Molecularweight (g mol^{-1})	390.89	933.76
UV absorption λmax (nm)	486	520
Charge	Cationic	Anionic

the BET technique (Brunauer–Emmett–Teller) using a Micrometric surface analyzer (Micro Active for TriStar II Plus 2.00). The Fourier Transform Infrared (FTIR) spectrum was recorded in the 4000–400 cm^{-1} range with a Perkin–Elmer 1730 FTIR, using the attenuated total reflection (ATR) technique. The method outlined by Azoulay et al. was used to find the point of zero charge (pH_{pzc}) [23], HCl and NaOH (0.1 M) were used to change the pH (pH_i) of aqueous solutions of NaCl (0.01 M) to a pH range of 2 to 12. Each sample (50 mL) was then given 0.05 g of MAC. The final pH (pH_f) of the solution was determined after stirring the dispersions for 24 h. A plot of ($pH_f - pH_i$) versus (pH_i) was used to determine the zero charge point.

Photocatalytic process

Before starting the study of the photocatalytic degradation of the dyes (BR18 and RR180) using the photocatalyst (MAC), the adsorption of the dyes on the photocatalyst was carried out in batch mode to confirm the adsorption equilibrium. The photocatalytic experiments were carried out in 500 mL cylindrical tubular reactor. Six ultraviolet (UV) light lamps (UVA, Philips TL8W Actinic BL) were used to irradiate this reactor, and they were arranged axially inside an aluminum cylinder. In order to maintain proper agitation of the photocatalyst in solution, ambient air was supplied to the system via a pump from the bottom of the reactor. The parameters studied for the photocatalytic degradation of dyes are various photocatalyst dosages (between 0.25 and 0.75 g L^{-1}) and a dye solution with a pH between 4 and 10 are added to each dye's initial concentration solution, which ranges from 50 to 200 mg L^{-1}. The samples were centrifuged for 5 min at 6000 rpm and the concentration of the supernatant solution was measured at wavelengths of 486 and 520 for RR18 and BR180 using a Hach DR-3900 type UV–visible spectrophotometer. The bleaching efficiency was calculated using Eq. 1:

$$R(\%) = [(C_0 - C_e)/C_0] \times 100 \quad (1)$$

here C_0 and C_e (mg L^{-1}) are the dye solution concentrations in the initial and equilibrium states, respectively.

The reuse of the photocatalyst was examined under the determined optimal conditions; this process was carried out using a magnetic field, as presented in Fig. S2.

To study in more detail the main reactive species responsible for the photocatalytic degradation of dyes (BR18 and RR180), trapping experiments were carried out in the presence of different sacrificial agents such as isopropanol (IPA), ascorbic acid (ASC), ethylene diaminetetraacetate (EDTA) and silver nitrate ($AgNO_3$) are used as scavengers of hydroxyl radicals ($HO^{\cdot}$), super oxide radicals ($O_2^{\cdot -}$), holes (h^+) and electrons (e^-) with a concentration of 4mM for each agent [24].

Results and discussion

Characterization of MAC

The X-ray diffraction pattern of MAC is shown in Fig. 1. It is clear from Fig. 1 that the MAC pattern shows the characteristic peaks related to the standard XRD pattern of cubic magnetite Fe_3O_4, these peaks at 2 theta of 30°0.18 (220), 35°0.54 (311), 43°0.21 (400), 54°0.00 (422), 57°0.16 (511) and 62°0.78 (440) [25–27], confirming the presence of pure, crystalline and spinel-structured Fe_3O_4. The infrared analysis spectrum of MAC is shown in Fig. 2, this spectrum shows the presence of different carbon and oxygen functional groups characteristic of the photocatalyst surface.

Fig. 3 shows heterogeneous pores were clearly observed on the surface of MAC and were organized by a group of honeycomb structures, the presence of these open and heterogeneous cylindrical pores are the origin of the large specific surface area. Fig. S3 shows the elemental composition of MAC obtained by EDX analysis, this analysis confirms the presence of carbon with a high content (C, 75.14%) and elements such as oxygen (O, 16.55%) and iron (Fe, 5.9%) in the structure of MAC. The adsorption–desorption isotherm of MAC (Fig. 4) is a type IV isotherm, according to the IUPAC classification, with an H4 type hysteresis loop connected to monolayer–multilayer adsorption followed by capillary condensation in tiny slot-shaped holes of uniform size existing at intermediate and high gauge pressures.The average pore diameter, total volume, and BET specific surface area of MAC were each 4.535 nm, 0.520 $cm^3\ g^{-1}$, and 837.357 $m^2\ g^{-1}$. MAC is a mesoporous material since the mean diameter of the pores (d = 4.535 nm) is situated in the mesopore area

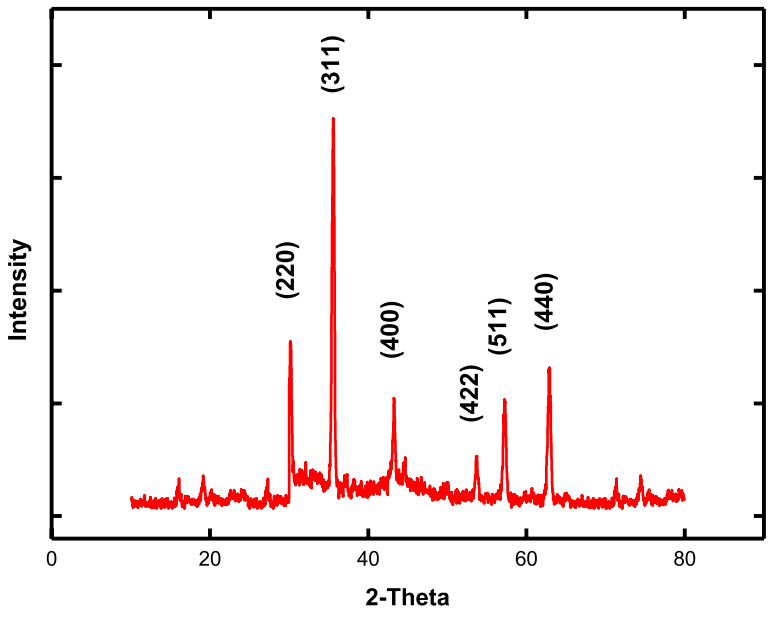

Fig. 1 XRD results of MAC

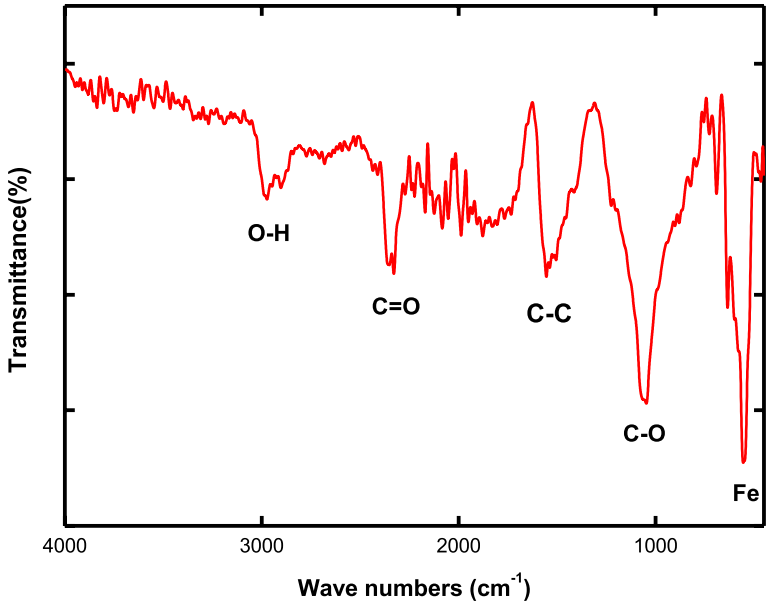

Fig. 2 FTIR spectra of MAC

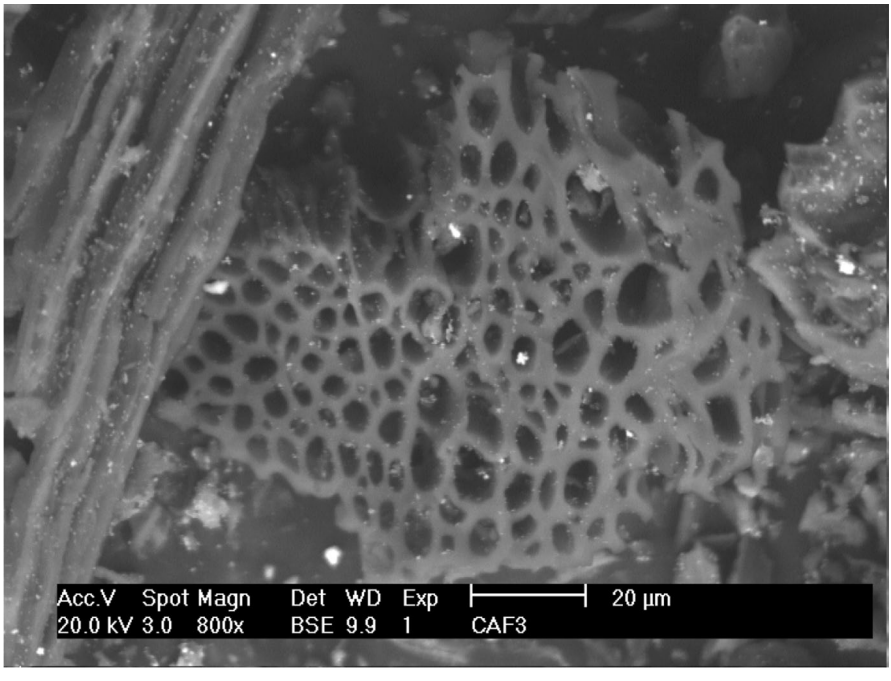

Fig. 3 SEM image of MAC

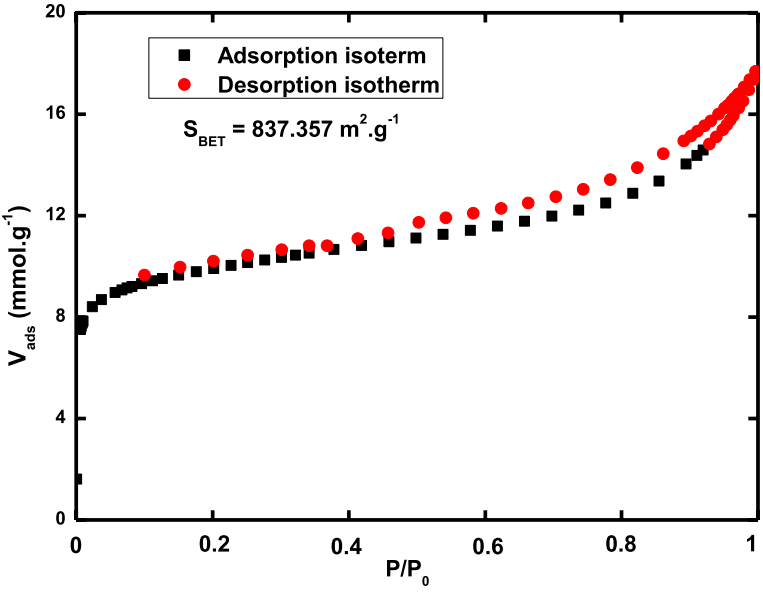

Fig. 4 Adsorption/desorption isotherm of MAC

(2 nm < d < 50 nm). Fig. S4 shows the change of zeta potential depending on pH between 3 and 11. The zeta potential of MACincreased with the increased pH values which was positively charged about over 6.8. These results from the characterization supported the effectiveness of the magnetic activated carbon preparation.

Research on dye degradation by photocatalysis

Effect of pH on the photocatalytic activity of MAC

The effect of solution pH in the range of 4 to 10 was studied on the degradation of BR18 and RR180 dyes with an initial concentration of 50 mg L^{-1} after 60 min using magnetic activated carbon under UVA light. The results presented in Fig. 5 show that the rate of degradation of BR18 is greater than that of RR180 over the entire pH range studied. A pseudo stabilization of BR18 dye degradation rate was observed with degradation efficiencies of 87.33%, 88.37%, 89.11% and 79.15% for solution pH values of 4, 6, 8 and 10. On the other hand, for the second dye (RR180) there is a significant effect of the pH of the solution on the photocatalytic activity of MAC. Fig. 5 illustrates the decolorization effectiveness of RR180 is slightly increased by raising pH from 4 to 6. It is clearly observed that the maximum degradation rate occurs at a neutral pH equal to 6 with a percentage of 68.65%. At the neutral-base range, the rate of decolorization of RR180 decreased as the pH of the solution increased. The pH of the MAC's point of zero charge (pH_{PZC}), which was around 6.8, can explain this behavior [6] as presented in Fig. S4, specifying that the

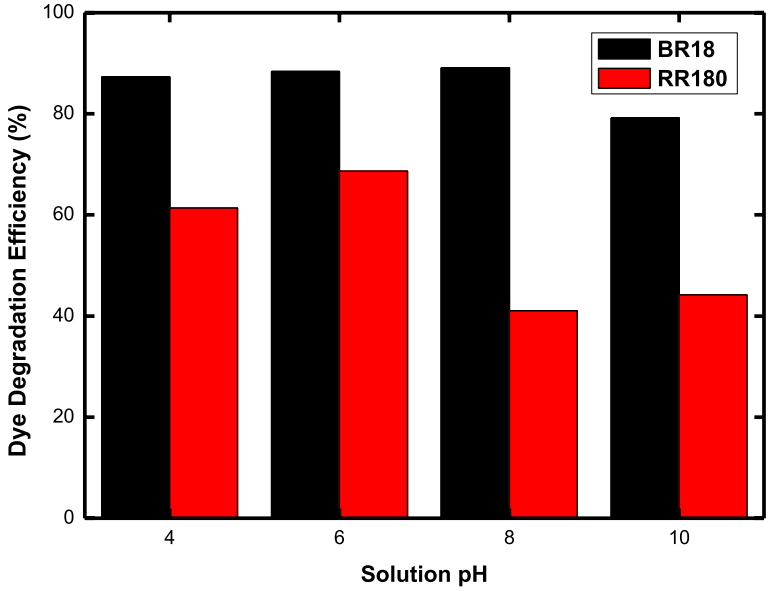

Fig. 5 Effect of pH values on the degradationefficiency of dyes. [$C_0 = 50$ mg L^{-1}; Dose = 0. 75 g L^{-1}; pH = 4, 6, 8 and 10; T = 20 °C]

surface of the photocatalyst has a negative charge in alkaline pH ($pH > pH_{PZC}$) and a positive charge in acid medium ($pH < PH_{PZC}$) [28]. As the pH increased, negative charges were induced on the photocatalyst surface, causing alkalinity in the solution [29, 30]. Electrostatic forces caused anionic dyes like (RR180) to be repelled from the photocatalyst surface, which decreased the surface's capacity to adsorb contaminating molecules as well as their contact with it. As a result of the prior disruptionscaused by the rise in pH of the solution, the degradation of the pollutant by the active radicals was also decreased. However, by decreasing the pH and making the solution acidic, positive charges were brought about on the photocatalyst surface [29, 30]. In contrast to the prior instance, anionic dye (RR180) was adsorbable on the photocatalyst surface thanks to electrostatic forces. The degradation of the dye (RR180) by the photocatalyst was improved as a result of the rise in the adsorption of polluting molecules on the photocatalyst surface and the decrease in disruptions brought on by the drop in pH of the solution [7, 31]. Similar resultes have been seen when BR18 and RR180 are photocatalytically degraded by various catalysts [32, 33]. For the two dyes, BR18 and RR180, the ideal pH values were found to be pH = 6.

Effect of MAC amount

The active photocatalytic sites are represented by the amount of catalyst in the solution. In this investigation, with a starting concentration of 50 mg L^{-1}, experiments were conducted to determine the impact of photocatalyst concentration on the photocatalytic degradation of the two dyes, BR18 and RR180. The effect of the MAC

dosage is determined in the range of 0.25 to 0.75 g $L^{-1}$for the photocatalytic degradation of BR18 and RR180 dyes, and the results are shown in Fig. 6. The results showed that the decoloration of BR18 dye was more effective than RR180 dye regardless of MAC dose. When the photocatalyst concentration is increased from 0.25 to 0.75 g L^{-1}, the percentage of dye degradation for RR180 and BR18 rises from 29 to 72.83% and 67.95 to 97.05%. This effect can be explained by theconsidering that as the dose of photocatalyst was increased, UVA light absorption improved, increasing the rate of photodegradation [34], and can be attributed to the increase in the transfer surface available. With high ratios of the solid to liquid ratio. Indeed, if the mass of the catalysts in the solution increases, the sites become more and morenumerous and consequently, the probability of encounter of the molecules of the dyes, with a site becomes more important [35]. The photocatalytic degradation of the two dyes (BR18 and RR180) by a variety of catalysts has been shown to have a comparable behavior [32, 36]. Therefore, the optimal amount of MAC for the degradation of the two dyes was determined to be 0.75 g L^{-1}.

Effect of initial dye concentration on MAC activity

In contrast to the other parameters, Figs. 7, 8 illustrates the effect of different dye concentrations ranging from 50 to 200 mg L^{-1}as a significant parameter on the effectiveness of dye degradation under UVA radiation. As the initial dye concentration increases, it is evident from Figs. 7, 8 that both dyes' degradation efficiencies gradually decline. The rate of degradation of the BR18 dye (Fig. 7) goes from 97.40% at 50 mg L^{-1} down to 49.74% at 200 mg L^{-1}. The increase in

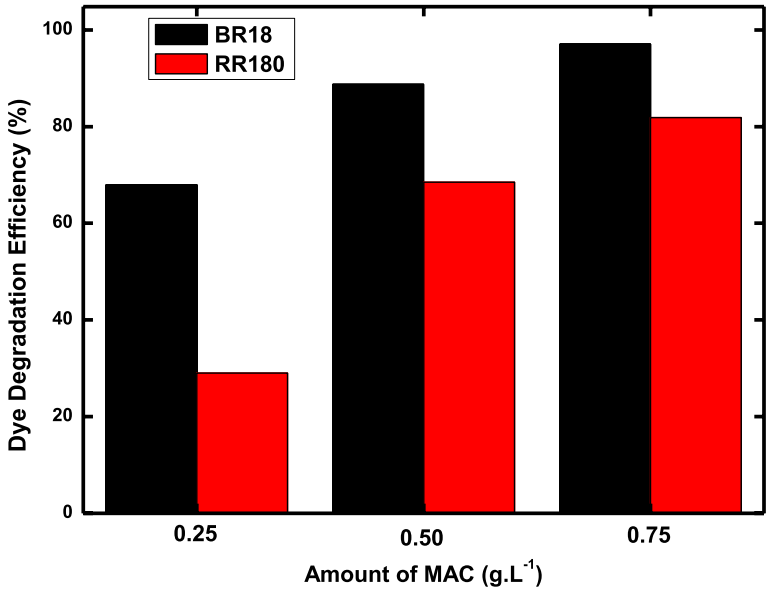

Fig. 6 Effect of MAC amount on thedegradationefficiency of dyes. [C_0 = 50 mg L^{-1}; Dose = 0.25; 0.50 and 0. 75 g $L.^{-1}$; pH = 6; T = 20 °C]

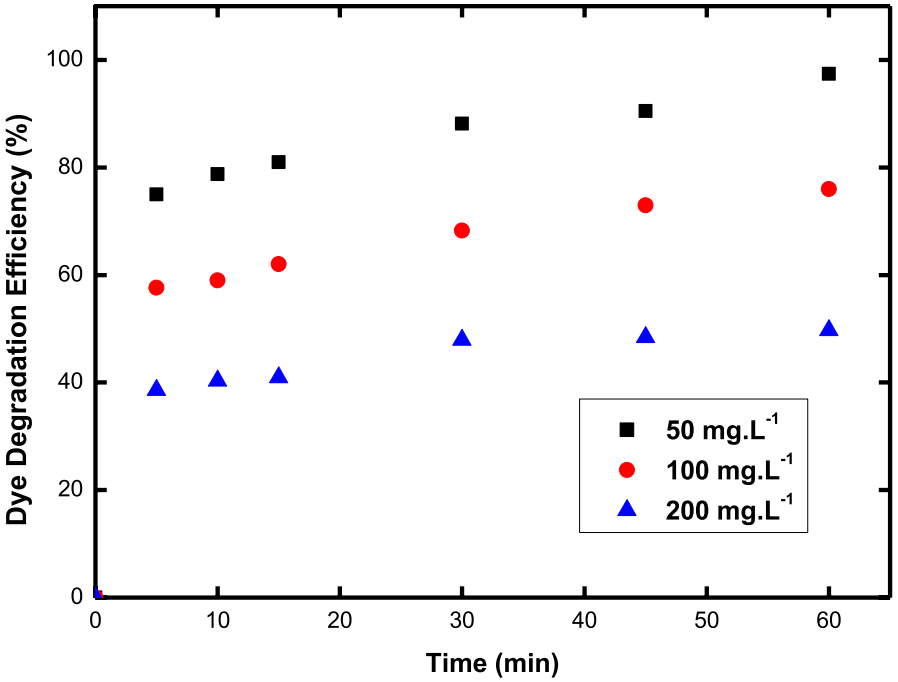

Fig. 7 Effect of initial dye concentration on the degradationefficiency of BR18 dye. [C_0 = 50, 100 and 200 mg L^{-1}; Dose = 0. 75 g L^{-1}; pH = 6; T = 20 °C]

initial RR180 dye concentration had a comparable effect (Fig. 8). After 60 min, tests with initial dye concentrations of 50 mg L^{-1}, 100 mg L^{-1}, and 200 mg L^{-1} revealed that the RR180 dye degraded at rates of 72.20%, 41.92%, and 33.43%. Similar effects have been seen when the two dyes (BR18 and RR180) were photocatalytically deraded by different catalysts [33, 36, 37]. As initial dye concentration increased the rate of degradation for both types of dyes decrease. The Beer–Lambert equation, which predicts that the rate of photocatalytic degradation decreases with a decrease in photons reaching the catalyst as the dye concentration rises and a reduction in the length of the photon path from the light source with intense concentration in the solution, can be used to explain this [38]. As illustrated in Table 2, the apparent first-order model is what emerged from kinetic analysis of the degradation process of the dyes BR18 and RR180, the rate constant of the apparent first-order model (k_{app}) decreased with the increase in dye content, an increase in the molecules (BR18 and RR180) that bind to the surface of the photocatalyst and stay out of direct contact with hydroxyl radicals (OH·) orholes (VB) could be the reason for this. On the other hand, the mass transfer phenomena may be able to control the reaction between the dye and the hydroxyl radicals (OH·), suggesting that the reserved effects are amplified as the dye concentration rises. However, the dye's photogenerated holes in the presence of a (OH·) scavenger were observed [39].

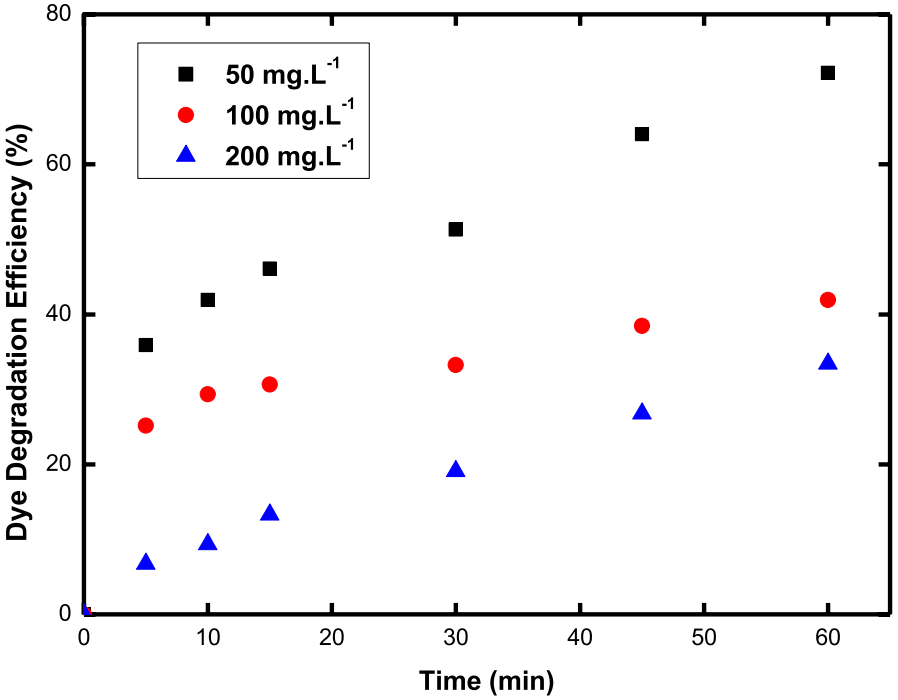

Fig. 8 Effect of initial dye concentration on the degradationefficiency of RR180 dye. [C_0 = 50, 100 and 200 mg L^{-1}; Dose = 0. 75 g L^{-1}; pH = 6; T = 20 °C]

Identification of reactive species of photocatalytic activity

To study in more detail the main reactive species responsible for the photocatalytic degradation of dyes (BR18 and RR180), trapping experiments were carried out in the presence of different sacrificial agents such as isopropanol (IPA), ascorbic acid (ASC), ethylene diamine tetraacetate (EDTA) and silver nitrate ($AgNO_3$) are used as scavengers of hydroxyl radicals ($HO^{\cdot}$), super oxide radicals ($O_2^{\cdot -}$), holes (h^+) and electrons (e^-) with a concentration of 4 mM for each agent [24, 40, 41]. As shown in Fig. 9, the photocatalytic activity decreased significantly in the presence of silver nitrate and ascorbic acid compared to the initial activity without adding scavengers for both dyes. This suggests that super oxide radicals ($O_2^{\cdot -}$) and electrons (e^-) are the main active species and play a major role in the photocatalytic degradation of dyes (BR18 and RR180) by magnetic activated carbon (MAC) under UVA light irradiation. Thus, the results obtained indicate that the order of the photoactive species generated is $e^- > O_2^{\cdot -} > h^+ > HO^{\cdot}$.

Mechanism of photo catalysis

The process of photocatalytic degradation of dyes by magnetic activated carbon occurs in several stages. Under UVA light irradiation, electrons (e^-) in the valence

Table 2 Kinetic parameters for the photocatalytic degradation of dyes using MAC

Dye	Basic Red 18 (BR18)					Reactive Red 180 (RR180)				
C_0 (mg L^{-1})	C_{exp} (mg L^{-1})	C_{cal} (mg L^{-1})	Standard error	k_{app} (min^{-1})	R^2	C_{exp} (mg L^{-1})	C_{cal} (mg L^{-1})	Standard error	k_{app} (min^{-1})	R^2
50	48.75	50.58	1.83	0.037	0.892	48.21	48.93	0.72	0.015	0.974
100	103.24	104.38	1.14	0.011	0.992	96.14	96.71	0.57	0.006	0.971
200	197.50	198.29	0.79	0.004	0.868	196.24	197.02	0.78	0.004	0.996

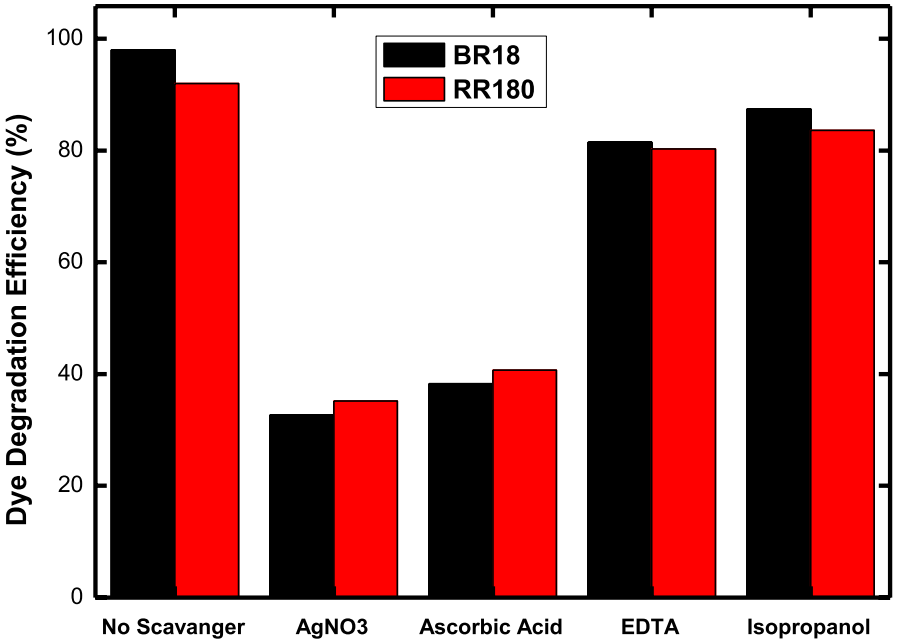

Fig. 9 Effect of scavengers on photo degradation of dyesunder UVA light. [C_0 = 50 mg L^{-1}; Dose = 0.75 g L^{-1}; pH = 6; [Agent] = 4 mM; T = 20 °C]

band (VB) are excited and move toward the conduction band (CB), generating holes (h^+) in the valence band (VB). The generated photo electrons combine with surface adsorbed oxygen on the MAC to form anionic super oxide radicals ($O_2^{\cdot -}$). The electrons also react with water and oxygen to form hydro peroxide ($HO_2^{\cdot}$) (Eq. 6) and H_2O_2 (Eqs. 4, 7). These radicals are responsible for the oxidation of dyes. Meanwhile, holes in the valence band (VB) of CAM absorb electrons from OH^- groups to form highly reactive hydroxyl radicals ($^{\cdot}OH$) [42]. These radicals and holes oxidize the dye, resulting in the production of various degraded products.

A proposed mechanism for the detailed reactions that occur on the MAC surface to degrade BR18 and RR180 molecules is presented below.

$$MAC\left(Fe_3O_4\right) + hv \rightarrow MAC\left(Fe_3O_4\right)\left(CB_{e-} + VB_{h+}\right) \tag{2}$$

$$MAC\left(Fe_3O_4\right) + \left(CB_{e-}\right) + O_2 \rightarrow MAC\left(Fe_3O_4\right) + O_2^{\cdot -} \tag{3}$$

$$2\,O_2^{\cdot -} + 2\,H_2O \rightarrow H_2O_2 + 2OH^- + O_2 \tag{4}$$

$$MAC\left(Fe_3O_4\right) + \left(VB_{h+}\right) + H_2O \rightarrow MAC\left(Fe_3O_4\right) + {}^{\cdot}OH + H^+ \tag{5}$$

$$O_2^{\cdot -} + H^+ \rightarrow HO_2^{\cdot} \tag{6}$$

$$HO_2^{\cdot} + \left(CB_{e-}\right) + H^+ \rightarrow H_2O_2 \tag{7}$$

$$Dye + hv \rightarrow Dye^* \tag{8}$$

$$Dye^* + MAC\left(Fe_3O_4\right) + \left(VB_{h+}\right) \rightarrow Dye^{+\cdot} + MAC\left(Fe_3O_4\right) \tag{9}$$

$$Dye^{+\cdot} + {}^{\cdot}OH / O_2^{\cdot -} \rightarrow CO_2 + H_2O \tag{10}$$

Reusability of the photocatalyst (MAC)

After the photocatalytic reaction, the produced photocatalyst could also be effortlessly removed from the solution using a magnet. Considering this property, the reusability of the photocatalyst was realized by studying its photocatalytic stability during five cycles under appropriate conditions determined for the two dyes. The proportion of dye degradation following each term of reuse is shown in Fig. 10. The proportion of BR18 degradation was discovered to range between 100

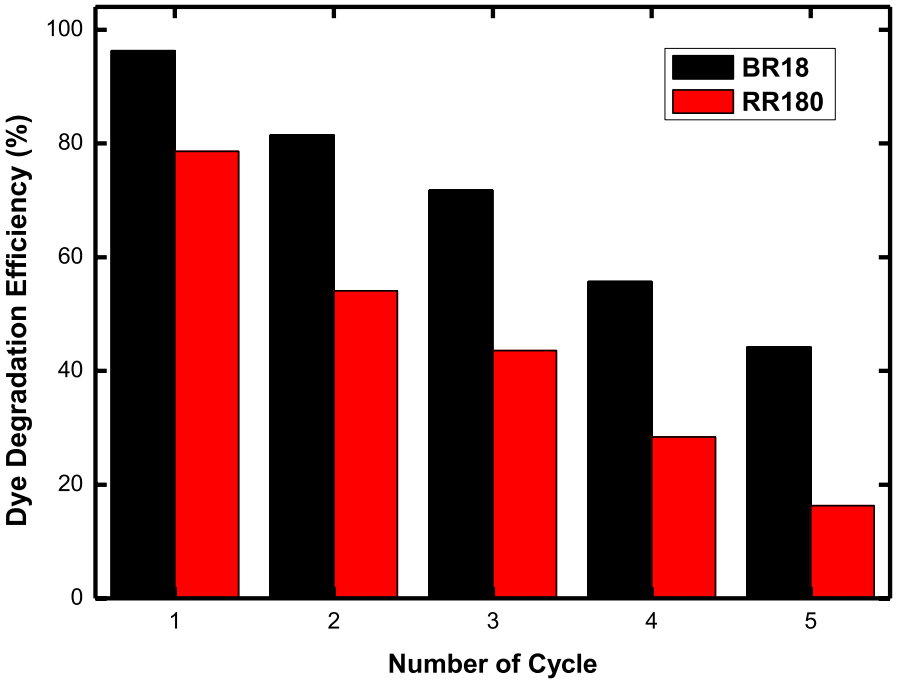

Fig. 10 Reuse of the MAC catalyst in the degradation of dyes. [$C_0 = 50$ mg L^{-1}; Dose = 0. 75 g L^{-1}; pH = 6; T = 20 °C]

and 82% during the first cycles before approaching 45% during the following five cycles. Regeneration data for the RR180 dye show that the efficiency of degradation decreased after each reuse cycle. The loss of photocatalyst that occurs inevitably after recovery from a magnetic field may be the cause of the drop in dyedegradation efficiency observed in reuse studies [43]. The photocatalyst regeneration experiments revealed that BR18 dye may be reused more successfully than RR180 dye, demonstrating the great selectivity of MAC for the degradation of cationic dyes.The reusability test findings indicate that the MAC has the potential to be reused in several treatment cycles.

Comparison of MAC with photocatalytic treatment systems

In this study, magnetic activated carbon was used as a photocatalyst under UVA light to examine the effectiveness of photocatalytic degradation of two types of dyes (BR18 and RR180). Table 3 compares the optimal circumstances attained in this investigation to those in other studies Eshagni et al. Bleached RR198 by a photocatalytic method (UV light) using TiO_2/AC nanocomposite. With a dye concentration of 100 mg L^{-1} and 1 g L^{-1} of catalyst, 97% of the solution had been eliminated after the 20 h reaction period. Chandraboss et al. used the AC/$BiSiO_2$ supported catalyst to degrade the MG dye in a photocatalytic system under UV light. In their work, adding 2.5 g L^{-1} of catalyst to the solution with a concentration of 36 mg L^{-1} resulted in a dye degradation efficiency of 95% for 75 min. Polat et al. studied the efficiency of photocatalytic degradation of BR18 and RR180 dyes using a synthesized material which is CuO under UVA light. They were able to attain maximum reduction efficiencies of 94.34% and 100% for BR18 and RR180 dyes, respectively, by adding 0.5 g L^{-1} of catalyst in a concentration solution of 10 mg L^{-1}, at neutral pH equal to 6 for 180 min. Eskikaya et al. studied the photocatalytic degradation of RR180 under UVA light by a photocatalyst obtained from sintered eggshells. When 1 g L^{-1} of catalyst was added to a solution with a concentration of 5 mg L^{-1}, the maximum degradation rate was determined to be 95.79% at neutral pH of 6 for 180 min.

According to Table 3, magnetic activated carbon obtained from the fruit shell of the Brachychiton populneus could be employed as an improved catalyst for the degradation of organic contaminants. Additionally, the synthesis of MAC is simple to do. And reproducible, therefore, it can be considered as an active, inexpensive, easily separable and stable photocatalyst.

Conclusion

In the present study, a magnetic activated carbon (MAC) was prepared from Brachychiton populneus fruit shell as a novel precursor for the photocatalytic degradation of two types of dyes, one cationic (BR18) and the other anionic (RR180) under UVA light source. The characterization results show the presence of Fe_3O_4 magnetic phase on the surface of MAC, the BET specific surface area, total pore volume and average pore diameter of CAM were 837.357 m^2 g^{-1}, 0.520 cm^3 g^{-1}

Table 3 Copmarison with other works

Photocatalyst	Dye	Conditions	Removal efficiency (%)	Light source	References
TiO_2–AC nano-composite	RR198	Dye consantration: 100 mg L^{-1}, catalyst amount: 1 g L^{-1}, time:20 h	97	UV light	[44]
AC-$BiSiO_2$	MG	Dye consantration: 36 mg L^{-1}, catalyst amount: 2 5 g L^{-1}, time: 75 min	95	UV (365 nm)	[45]
CuO powder	BR18 RR180	Dye consantration: 10 mg L^{-1}, catalyst amount: 0.5 g L^{-1}, time: 180 min, pH: 6 H_2O_2 concentration: 1.11 mg L^{-1}	94.34 for BR18 100 for RR180	450-nm multimode semiconductor diode laser	[32]
$Mg_{0.2}Zn_{0.8}Sm_{0.2}Fe_{1.8}O_4$	RhB	Dye consantration: 5 mg L^{-1}, catalyst amount: 25 g L^{-1}, time: 270 min	94.13	Visible light	[46]
Waste chicken eggshells sintered at 900 °C	BR18 RR180	Dye consantration: 5 mg L^{-1}, catalyst amount: 1 g L^{-1}, time: 180 min, pH: 6.8	100 for BR18 97.9 for RR180	Visible light	[33]
Nano-HAp	RBBR	Dye consantration: 10 mg L^{-1}, catalyst amount: 0.5 g L^{-1}, time: 120 min	80	UV light	[47]
MAC	BR18 RR180	Dye consantration: 50 mg L^{-1}, catalyst amount: 0.75 g L^{-1}, time: 60 min, pH: 6	100 for BR18 82 for RR180	UVA light	This study

and 4.535 nm, which confirms a mesoporous material.For an initial dye concentration of 50 mg L^{-1}, the optimal values of the parameters studied are: pH of the solution (8 for BR18 and 6 for RR180) and 0.75 g L^{-1} quantity of MAC with a degradation rate of 100% and 82% for BR18 and RR180, respectively. The apparent first-order model of the reaction process is supported by kinetic studies of the degradation reaction of the dyes BR18 and RR180. Super oxide radicals and electrons are the main active species and play a major role in the photocatalytic degradation of dyes by magnetic activated carbon under UVA light irradiation. MAC demonstrated satisfactory reusability as a photocatalyst for five cycles. The results of the study of the photocatalytic degradation of the two dyes by MAC from the shell of the fruit Brachychiton populneus showed that this photocatalyst is very effective in the treatment of water polluted by organic pollutants.

Supplementary Information The online version contains supplementary material available at https://doi.org/10.1007/s11144-024-02648-4.

Data availability The authors declare that the data supporting the findings of this study are available within the article and its Supplementary Information files.

References

1. Sharififard H, Nabavinia M, Soleimani M (2017) Evaluation of adsorption efficiency of activated carbon/chitosan composite for removal of Cr (VI) and Cd (II) from single and bisolute dilute solution. Adv Env Technol 2(4):215–227
2. Gupta VK, Nayak A (2012) Cadmium removal and recovery from aqueous solutions by novel adsorbents prepared from orange peel and Fe_2O_3 nanoparticles. Chem Eng J 180:81–90
3. Dutta M, Bhattacharjee S, De S (2020) Separation of reactive dyes from textile effluent by hydrolyzed polyacrylonitrile hollow fiber ultrafiltration quantifying the transport of multicomponent species through charged membrane pores. Sep Purif Technol 234:116063
4. Bilici Z, Bouchareb R, Sacak T, Yatmaz HC, Dizge N (2021) Recycling of TiO_2-containing waste and utilization by photocatalytic degradation of a reactive dye solution. Water Sci Technol 83(5):1242–1249
5. Kshirsagar AS, Gautam A, Khanna PK (2017) Efficient photo-catalytic oxidative degradation of organic dyes using $CuInSe_2/TiO_2$ hybridhetero-nanostructures. J Photochem Photobiol, A 349:73–90
6. Bouider B, Rida K (2022) Development of biomass activated carbon using full factorial design for the removal of methyl orange from aqueous solution. Desalin Water Treat 267:240–252
7. Mahmoodi NM, Abdi J, Taghizadeh M, Taghizadeh A, Hayati B, Shekarchi AA, Vossoughi M (2019) Activated carbon/metal-organic framework nanocomposite: preparation and photocatalytic dye degradation mathematical modeling from wastewater by least squares support vector machine. J Environ Manage 233:660–672
8. Liang R, Luo S, Jing F, Shen L, Qin N, Wu L (2015) A simple strategy for fabrication of Pd@MIL-100 (Fe) nanocomposite as a visible-light-driven photocatalyst for the treatment of pharmaceuticals and personal care products (PPCPs). Appl Catal B 176:240–248
9. Sibhatu AK, Weldegebrieal GK, Sagadevan S, Tran NN, Hessel V (2022) Photocatalytic activity of CuO nanoparticles for organic and inorganic pollutants removal in wastewater remediation. Chemosphere. https://doi.org/10.1016/j.chemosphere.2022.134623
10. Jain M, Yadav M, Kohout T, Lahtinen M, Garg VK, Sillanpää M (2018) Development of iron oxide/activated carbon nanoparticle composite for the removal of Cr (VI), Cu (II) and Cd (II) ions from aqueous solution. Water Resour Ind 20:54–74

11. Al-Mamun MR, Kader S, Islam MS, Khan MZH (2019) Photocatalytic activity improvement and application of UV-TiO_2 photocatalysis in textile wastewater treatment: a review. J Environ Chem Eng 7(5):103248
12. Roy N, Chakraborty S (2021) ZnO as photocatalyst: an approach to waste water treatment. Mater Today: Proc 46(14):6399–6403
13. Li JX, Zhang RL, Pan ZJ, Liao Y, Xiong CB, Chen ML, Huang R, Pan XH, Chen Z (2021) Preparation of CdS@Cphotocatalyst using phytoaccumulation Cd recycled from contaminated wastewater. Front Chem 9:717210
14. Da Silva MP, de Souza ZSB, Cavalcanti JVFL et al (2021) Adsorptive and photocatalytic activity of Fe_3O_4-functionalized multilayer grapheme oxide in the treatment of industrial textile wastewater. Environ Sci Pollut Res 28:23684–23698
15. Wang JL, Wang C, Lin W (2012) Metal–organic frameworks for light harvesting and photocatalysis. ACS Catal 2(12):2630–2640
16. Maleki S, Falaki F, Karimi M (2019) Synthesis of SDS micelles-coated Fe_3O_4/SiO_2magnetic nanoparticles as an excellent adsorbent for facile removal and concentration of crystal violet fromnatural water samples. J Nanostruct Chem 9:129–139
17. Liu N, Huang W, Zhang X, Tang L, Wang L, Wang Y, Wu M (2018) Ultrathin grapheme oxide encapsulated in uniform MIL-88A (Fe) for enhanced visible light-drivenphotodegradation of RhB. Appl Catal B 221:119–128
18. Lai SY, Ng KH, Cheng CK, Nur H, Nurhadi M, Arumugam M (2021) Photocatalytic remediation of organicwaste over Keggin-based polyoxometalate materials: a review. Chemosphere 263:128244
19. DaiLamTran VHL, Pham HL, Hoang TMN, Nguyen TQ, Luong TT, Ha PT, Nguyen XP (2010) Biomedical and environmental applications of magnetic nanoparticles. Adv Nat Sci: Nanosci Nanotechnol. https://doi.org/10.1088/2043-6262/1/4/045013
20. Liu WJ, Jiang H, Yu HQ (2015) Development of biochar-based functional materials: toward a sustainable platform carbon material. Chem Rev 115(22):12251–12285
21. Cazetta AL, Pezoti O, Bedin KC, Silva TL, Paesano Junior A, Asefa T, Almeida VC (2016) Magnetic activated carbon derived from biomass waste by concurrent synthesis: efficient adsorbent for toxicdyes. ACS Sustain Chem Eng 4(3):1058–1068
22. Feiqiang G, Xiaolei L, Xiaochen J, Xingmin Z, Chenglong G, Zhonghao R (2018) Characteristics and toxicdye adsorption of magnetic activated carbon prepared from biomass waste by modified one-step synthesis. Colloids Surf A 555:43–54
23. Azoulay K, Bencheikh I, Moufti A, Dahchour A, Mabrouki J, El Hajjaji S (2020) Comparative study between static and dynamic adsorption efficiency of dyes by the mixture of palm waste using the central composite design. Chem Data Collect 27:100385
24. Haounati R, Alakhras F, Ouachtak H, Saleh TA, Al-Mazaideh G, Alhajri E, Jada A, Hafid N, Addi AA (2023) Synthesized of zeolite@ Ag_2O nanocomposite as superb stability photocatalysis toward hazardous rhodamine B dye from water. Arab J Sci Eng. 48(1):169–79
25. Datta D, KerkezKuyumcu Ö, Bayazit ŞS, Abdel Salam M (2017) Adsorptive removal of malachite green and Rhodamine B dyes on Fe_3O_4/activated carbon composite. J Dispers Sci Technol 38(11):1556–1562
26. Baghdadi M, Ghaffari E, Aminzadeh B (2016) Removal of carbamazepine from municipal wastewater effluent using optimally synthesized magnetic activated carbon: adsorption and sedimentation kinetic studies. J Environ Chem Eng 4(3):3309–3321
27. Cheng X, Ji Q, Sun D, Zhang J, Chen X, He H, Zhang L (2022) A comparative study on adsorption behavior of iodinated X-ray contrast media iohexol and amidotrizoic acid by magnetic-activatedcarbon. Environ Sci Pollut Res 29(30):45404–45420
28. Salehi M, Hashemipour H, Mirzaee M (2012) Experimental study of influencing factors and kinetics in catalytic removal of methylene blue with TiO_2 nanopowder. Am J Environ Eng 2(1):1–7
29. Yang C, You X, Cheng J, Zheng H, Chen Y (2017) A novel visible-light-driven In-basedMOF/grapheneoxidecomposite photocatalyst with enhanced photocatalytic activity toward the degradation of amoxicillin. Appl Catal B: Environ 200:673–680
30. Bagherzadeh SB, Kazemeini M, Mahmoodi NM (2020) A study of the DR23 dye photocatalytic degradation utilizing a magnetic hybrid nanocomposite of MIL-53 (Fe)/$CoFe_2O_4$: facile synthesis and kinetic investigations. J Mol Liq 301:112427
31. Sillanpää M, Ncibi MC, Matilainen A (2018) Advanced oxidationprocesses for the removal of naturalorganic matter from drinking water sources: a comprehensive review. J Environ Manage 208:56–76

32. Polat B, Bilici Z, Ozay Y, Kucukkara I, Dizge N (2022) Photocatalytic decolorization of BR18 and RR180 dyes by semiconductor diode laser using CuO for wastewater treatment. Water Air Soil Pollut 233(8):316
33. Eskikaya O, Gun M, Bouchareb R, Bilici Z, Dizge N, Ramaraj R, Balakrishnan D (2022) Photocatalytic activity of calcined chicken eggshells for Safranin and Reactive Red 180 decolorization. Chemosphere 304:135210
34. Ghasemi B, Anvaripour B, Jorfi S, Jaafarzadeh N (2016) Enhanced photocatalytic degradation and mineralization of furfural using UVC/TiO_2/GAC composite in aqueous solution. Int J Photoenergy. https://doi.org/10.1155/2016/2782607
35. Akyol A, Yatmaz HC, Bayramoglu M (2004) Photocatalytic decolorization of Remazol Red RR in aqueous ZnO suspensions. Appl Catal B 54(1):19–24
36. Eskikaya O, Ozdemir S, Tollu G, Dizge N, Ramaraj R, Manivannan A, Balakrishnan D (2022) Synthesis of two different zinc oxide nanoflowers and comparison of antioxidant and photocatalyticactivity. Chemosphere 306:135389
37. Eskikaya O, Isik Z, Arslantas C, Yabalak E, Balakrishnan D, Dizge N, Rao KS (2023) Preparation of hydrochar bio-based catalyst for fenton process in dye-containing waste water treatment. Environ Res 216:114357
38. Siong VLE, Lee KM, Juan JC, Lai CW, Tai XH, Khe CS (2019) Removal of methylene blue dye by solvothermally reduced grapheme oxide: ametal-free adsorption and photodegradation method. RSC Adv 9(64):37686–37695
39. Mahvi AH, Ghanbarian M, Nasseri S, Khairi A (2009) Mineralization and discoloration of textile wastewater by TiO_2 nanoparticles. Desalination 239(1–3):309–316
40. Ji P, Zhang J, Chen F, Anpo M (2009) Study of adsorption and degradation of acid orange 7 on the surface of CeO_2 under visible light irradiation. Appl Catal B 85:148–154
41. Yin M, Li Z, Kou J, Zou Z (2009) Mechanism investigation of visible light-induced degradation in a heterogeneous TiO_2/Eosin Y/Rhodamine B system. Environ Sci Technol 43:8361–8366
42. Coronado JM, Maira AJ, Martínez-Arias A, Conesa JC, Soria J (2002) EPR study of the radicals formed upon UV irradiation of ceria-based photocatalysts. J Photochem Photobiol A: Chem 150(1–3):213–21
43. El-Berry MF, Sadeek SA, Abdalla AM, Nassar MY (2021) Microwave-assisted fabrication of copper nanoparticles utilizing different counter ions: an efficient photocatalyst for photocatalytic degradation of safranin dye from aqueous media. Mater Res Bull 133:111048
44. Eshaghi A, Hayeripour S, Eshaghi A (2016) Photocatalytic decolorization of reactivered 198 dye by a TiO_2–activated carbon nano-composite derived from the sol–gel method. Res Chem Intermed 42:2461–2471
45. Chandraboss VL, Kamalakkannan J, Senthilvelan S (2015) Synthesis of AC-Bi@ SiO_2 nanocomposites phere for superiorphotoc atalyticactivity towards the photodegradation of malachite green. Can Chem Trans 3(4):410–429
46. Mansour SF, Wageh S, Al-Wafi R, Abdo MA (2021) Enhanced magnetic, dielectric properties and photocatalytic activity of doped Mg–Zn ferrite nanoparticles by virtue of Sm^{3+} role. J Alloy Compd 856:157437
47. Begum S, Narwade VN, Halge DI, Jejurikar SM, Dadge JW, Muduli S, Bogle KA (2020) Remarkable photocatalytic degradation of Remazol Brilliant Blue R dyeusing bio-photocatalyst 'nano-hydroxyapatite.' Mater Res Expr 7(2):025013
48. Lente G (2018) Facts and alternative facts in chemical kinetics: remarks about the kinetic use of activities, termolecular processes, and linearization techniques. Curr Opin Chem Eng 21:76–83